

The NOD2-RICK Complex Signals from the Plasma Membrane*[§]

Received for publication, June 29, 2006, and in revised form, March 5, 2007. Published, JBC Papers in Press, March 13, 2007, DOI 10.1074/jbc.M606242200

Patrick Lécine^{†1}, Sophie Esmiol^{§1,2}, Jean-Yves Métais^{‡3}, Cendrine Nicoletti[§], Claire Nourry[‡], Christine McDonald[¶], Gabriel Nunez[¶], Jean-Pierre Hugot^{||}, Jean-Paul Borg[‡], and Vincent Ollendorff^{§4}

From the [†]Centre de Recherche en Cancérologie de Marseille, UMR 599 INSERM-Institut Paoli-Calmettes-Université de la Méditerranée, 27 Boulevard Leï Roure, 13009 Marseille, France, [§]IMRN, INRA UMR 1111, Université Paul Cézanne Faculté de St. Jérôme Service 342, Avenue Escadrille Normandie Niemen, 13397 Marseille Cedex 20, France, the [¶]Department of Pathology, University of Michigan Medical School and Comprehensive Cancer Center, Ann Arbor, Michigan 48109, and ^{||}INSERM U763, Université Paris 7 UFR Médicale Denis Diderot, Assistance Publique-Hopitaux de Paris, Hôpital Robert Debré, 75019 Paris, France

NOD2 plays an important role in the innate immunity of the intestinal tract. By sensing the muramyl dipeptide (MDP), a bacterial wall component, NOD2 triggers the NF- κ B signaling pathway and promotes the release of proinflammatory cytokines such as interleukin-8. Mutations in *Nod2* (1007FS, R702W, G908R) impinge on NOD2 functions and are associated with the pathogenesis of Crohn disease, a chronic inflammatory bowel disease. Although NOD2 is usually described as a cytosolic receptor for MDP, the protein is also localized at the plasma membrane, and the 1007FS mutation delocalizes NOD2 to the cytoplasm (Barnich, N., Aguirre, J. E., Reinecker, H. C., Xavier, R., and Podolsky, D. K. (2005) *J. Cell Biol.* 170, 21–26; McDonald, C., Chen, F. F., Ollendorff, V., Ogura, Y., Marchetto, S., Lecine, P., Borg, J. P., and Nunez, G. (2005) *J. Biol. Chem.* 280, 40301–40309). In this study, we demonstrate that membrane-bound versions of NOD2 and Crohn disease-associated mutants R702W and G908R are capable of responding to MDP and activating the NF- κ B pathway from this location. In contrast, the 1007FS mutant remains unable to respond to MDP from the plasma membrane. We also show that NOD2 promotes the membrane recruitment of RICK, a serine-threonine kinase involved in NF- κ B activation downstream of NOD2. Furthermore, the artificial attachment of RICK at the plasma membrane provokes a constitutive and strong activation of the NF- κ B pathway and secretion of interleukin-8 showing that optimal RICK activity depends upon its subcellular localization. Finally, we show that endogenous RICK localizes at the plasma membrane in the THP1 cell line. Thus, our data suggest that NOD2 is responsible for the membrane recruitment of RICK to induce a regulated NF- κ B signaling and production of proinflammatory cytokines.

Resistance to infectious diseases relies on the ability of the organism to prevent the invasion of pathogens and to mount efficient and sustainable immune responses. Epithelial cells act as a fence against external aggressions by forming a barrier between the interior and the exterior of the body. When invasion of pathogens occurs despite this, innate and adaptive immune responses prepare to eradicate the intruders. Inflammatory bowel diseases (IBD)⁵ are due to concomitant genetic, epigenetic, and environmental factors that preclude the mounting of an adequate innate and adaptive immunity toward intestinal pathogens and/or commensal bacteria (3, 4). Crohn disease (CD) is one of the two major forms of IBD affecting Western countries (5). Candidate gene analysis has revealed *Nod2* as the first gene associated with CD susceptibility (6, 7), and multiple *Nod2* variants (more than 60) have been described so far, in particular the mutations R702W, G908R, and 1007FS have been identified in the genome of 30–40% of CD patients (8). NOD2 contains two amino-terminal caspase recruitment domains (CARDs), a central nucleotide oligomerization domain (NOD), and carboxyl-terminal leucine-rich repeats (LRRs) (9, 10). NOD2 is a general sensor for Gram-positive and Gram-negative bacteria because it is able to respond to MDP, a component of bacterial peptidoglycans (11, 12). The NOD2^{R702W}, NOD2^{G908R}, and NOD2^{1007FS} mutations are lying in proximity to or within the LRRs of NOD2 thought to be involved in MDP recognition (13). The CARDs are required for the binding to RICK (also called Ripk2), a serine-threonine kinase involved in the activation of the NF- κ B pathway through ubiquitinylation of IKK γ and phosphorylation of the I κ B kinases, which promotes the production of proinflammatory cytokines (10, 14, 15).

In CD patients, increased amounts of activated NF- κ B are evidenced in the inflamed epithelial tissues as well as increased

* The costs of publication of this article were defrayed in part by the payment of page charges. This article must therefore be hereby marked "advertisement" in accordance with 18 U.S.C. Section 1734 solely to indicate this fact.

[§] The on-line version of this article (available at <http://www.jbc.org>) contains supplemental Figs. S1–S3.

¹ Both authors contributed equally to this work.

² Supported by a MESR fellowship.

³ Present address: Hematology Branch, NHLBI, National Institutes of Health, Bldg. 10 CRC, Rm. 3-3216, 9000 Rockville Pike, Bethesda, MD 20892.

⁴ To whom correspondence should be addressed. Tel.: 33-491-28-28-66; E-mail: vincent.ollendorff@univ-cezanne.fr.

⁵ The abbreviations used are: IBD, inflammatory bowel diseases; CARD, caspase activation and recruitment domain; CD, Crohn disease; EGFP, enhanced green fluorescent protein; ECFP, enhanced cyan fluorescent protein; EYFP, enhanced yellow fluorescent protein; HEK293T, human embryonic kidney 293T cells; IL, interleukin; LAP, leucine-rich repeat and PDZ; MDCK, Madin-Darby canine kidney; MDP, muramyl dipeptide; myr, myristoylated; NOD, nucleotide oligomerization domain; TLR2, Toll-like receptor 2; WT, wild type; ELISA, enzyme-linked immunosorbent assay; FCS, fetal calf serum; PBS, phosphate-buffered saline; GFP, green fluorescent protein; MAPK, mitogen-activated protein kinase; LRR, leucine-rich repeats.

Membrane Signaling of NOD2 and RICK

amounts of proinflammatory cytokines secreted by lamina propria mononuclear cells such as tumor necrosis factor α and IL-1 β in response to lipopolysaccharide (16, 17). Furthermore, knock-in mice carrying two *1007fs* alleles (2939iC mutant) have an increased colonic inflammation when treated with dextran sulfate sodium (18), and stimulation of their bone marrow-derived macrophages with MDP produces a higher NF- κ B response, resulting in enhanced secretion of IL-1 β . This “gain-of-function” phenotype is further supported by the fact that *Nod2*^{-/-} mice do not develop an IBD-like phenotype, although they display innate and adaptive immune defects (19). For example, *Nod2*^{-/-} mice appear to be deficient in α -defensin production that may affect innate immunity responses and mucosal homeostasis with the commensal flora (19).

Strikingly, this gain of function hypothesis is in contrast with other studies indicating that the NOD2^{1007FS} mutation leads to a deficient NOD2 activity. Indeed, peripheral blood mononuclear cells from CD patients carrying the NOD2^{1007FS} mutation are unable to secrete proinflammatory chemokine IL-8 in response to MDP or peptidoglycan but are still able to respond to lipopolysaccharide (20, 21). Accordingly, in transfected cells, the NOD2-dependent NF- κ B activity in response to MDP is lost when the NOD2^{1007FS} mutant is expressed, suggesting that it acts as a loss-of-function mutant (12). Other common CD-associated mutants NOD2^{R702W} and NOD2^{G908R} exhibit an intermediate phenotype and induce NF- κ B to a smaller extent compared with wild type NOD2 (1, 12, 22).

Further studies performed by Watanabe *et al.* (23) with splenic macrophages of *Nod2*^{-/-} mice have highlighted a possible negative role of intact NOD2 on a Toll-like receptor 2 (TLR2) signaling pathway that may explain the increased inflammation observed with the NOD2^{1007FS} mutant. Because of its absence of response to MDP, NOD2^{1007FS} mutant may cause an excessive lymphocyte T helper type 1 (Th1) cytokine production by enhancing TLR2-mediated NF- κ B activation, particularly through the c-Rel subunit (23, 24).

Several models have been proposed to explain these numerous and sometimes conflicting experimental results on the biological effect of CD-associated *Nod2* mutations (25). The paradox may only be apparent, however, and the consequence of the CD-associated NOD2^{1007FS} mutation may be either a gain or a loss of function depending on the cellular or animal model and on the readout. In any case, a better understanding on the function of NOD2 at the molecular level within a specific cellular environment is needed.

Subcellular compartmentalization of signaling molecules at the plasma membrane is a common theme in signal transduction and a mean to bring specificity and regulation to signaling pathways. NOD2 is expressed in macrophages and epithelial cells (10, 26) where it binds to several partners, including RICK, TAK1 (27, 28) and Grim-19, CLAN, and caspase-1 (28, 29). Recently it has been shown that a pool of NOD2 localizes at the plasma membrane in HEK293 cells and in a polarized epithelial cell model (Caco-2 cells), where it is associated with Erbin, a basolateral protein belonging to the leucine-rich repeat and PDZ family (1, 2, 30). Furthermore, the activity of NOD2 proteins correlates with their ability to localize to the plasma membrane because the NOD2^{1007FS} mutant, delocalized to the cyto-

plasm, is unable to properly activate NF- κ B in response to MDP (1). In this study we have further investigated the activity of NOD2 that triggers NF- κ B activation at the plasma membrane. We demonstrate that an enforced localization of NOD2 at the plasma membrane maintains its NF- κ B activity. We also show that NOD2 recruits RICK at the plasma membrane, thus promoting NF- κ B activation and IL-8 secretion. Taken together, these data emphasize the importance of membrane localization of NOD2 and RICK to trigger an optimal NF- κ B activation.

EXPERIMENTAL PROCEDURES

Cell Culture—HEK293T and MDCKII cells were grown in Dulbecco's modified Eagle's medium containing 10% FCS deplete, 100 units/ml penicillin, and 100 μ g/ml streptomycin sulfate. Caco-2 cells were grown in Dulbecco's modified Eagle's medium containing 20% FCS deplete, 2 mM glutamine, 100 units/ml penicillin, and 100 mg/ml streptomycin sulfate. HCT116 were grown in McCoy's medium containing penicillin and streptomycin and 10% FCS. THP1 cells were grown in RPMI1640 supplemented with 10% FCS deplete. Cell transfections were performed using FuGENE 6 (Roche Applied Science) or Lipofectamine 2000 (Invitrogen) according to the manufacturer's recommendations.

Expression Vectors—All cloning experiments were performed using the GatewayTM system (Invitrogen). All cDNAs were cloned into pDONRTM201 or pDONRTM/Zeo from PCR products. All cDNAs were fully sequenced in pDONR and subsequently shuttled into pEGFP-GW, pMyrEGFP-GW, pRK5myc-GW, pECFP-GW, or pEYFP-GW. pECFP-GW and pEYFP-GW are described in Ref. 31. pEGFP-GW was constructed by subcloning a Gateway cassette into the XbaI and SalI sites of pEGFP-C1. pMyrEGFP-GW was created by cloning the PCR product (using pEGFP-C1 (Clontech) as a template and the following primers: Myr-EGFPFW, CGCGCTAGCAC-CATGGGCTGTGGCTGCAGCTCACACCCGGAAGATGT-GAGCAAGGGCGAGGAGCTGT, and Myr-EGFP-RV, GTT-ATCTAGATCCGGTGGATCC) into pEGFP-GW (NheI and XhoI). Mutations in NOD2 cDNA were introduced using the QuikChangeTM mutagenesis kit (Stratagene).

Biochemical Procedures—Cells were rinsed twice in cold PBS and lysed in buffer containing 50 mM HEPES, pH 7.5, 1 mM EGTA, 150 mM NaCl, 1.5 mM MgCl₂, 10% glycerol, 1% Triton X-100, supplemented with 1 mM phenylmethylsulfonyl fluoride, 1 mM orthovanadate, and Protease Inhibitors Mixture (Sigma). Triton-soluble proteins were recovered in the supernatant of a 20-min centrifugation at 13,000 \times g and at 4 $^{\circ}$ C. For cell fractionation, cells were lysed in hypotonic buffer (10 mM Tris, pH 7.4, 1 mM MgCl₂, 0.1 mM CaCl₂, 5 mM KCl) using a Dounce homogenizer (20 strokes). Sucrose and EDTA were added to the homogenate to a final concentration of 0.25 M and 1 mM, respectively, and nonhomogenized debris was removed by centrifugation at 3,500 \times g for 10 min at 4 $^{\circ}$ C. The supernatant was termed the hypotonic fraction. The pellet was then resuspended in lysis buffer for 10 min at 4 $^{\circ}$ C and centrifuged at 16,000 \times g for 10 min at 4 $^{\circ}$ C. The supernatant and the pellet were termed Triton X-100-soluble and Triton X-100-insoluble fractions, respectively.

Immunofluorescence and Confocal Microscopy—MDCKII cells were grown on Transwell™ filters, washed twice in PBS, 0.1 mM Ca²⁺, 1 mM Mg²⁺, and fixed for 20 min in 4% paraformaldehyde at 4 °C. Cells were permeabilized during 5 min with 0.5% Triton X-100 at room temperature and blocked in 0.25% gelatin for 1 h at room temperature. Antibodies diluted in the blocking buffer were incubated overnight at 4 °C. After four 15-min washes, the cells were incubated for 1 h at room temperature with secondary antibodies coupled to fluorescent probes. Cells were washed and filters were mounted in Dako (The Jackson Laboratory) for confocal microscopy analyses on an Olympus IX70 (Fluoview 500). For HEK293T and HCT116 cells, immunofluorescence labeling was done on coverslips 16–20 h following transfection. Coverslips were washed in PBS, fixed in 4% paraformaldehyde for 30 min, washed three times in PBS, permeabilized in Triton 0.2%, blocked in 3% bovine serum albumin/PBS one time, and incubated with an anti-Myc monoclonal antibody (9E10; 0.4 μg/ml). After 1 h of incubation and five washes in PBS, coverslips were incubated 45 min with a secondary goat anti-mouse antibody (highly cross-adsorbed) coupled to Alexa 594 (Molecular Probes). Finally, the cells were washed extensively and mounted in Dako (The Jackson Laboratory) or Vectashield for microscopic analysis on a Zeiss Axiovert 200M microscope. HEK293T or HCT116 expressing EGFP, ECFP, or EYFP fusion proteins were washed in PBS, fixed in 4% paraformaldehyde, washed in PBS, and mounted directly for microscopic analysis.

Antibodies and Reagents—Monoclonal anti-GFP (11814460001) and anti-Shc (610879) were purchased from Roche Applied Science and BD Biosciences, respectively. Monoclonal anti-Myc (9E10, Sc-40), rabbit polyclonal anti-RICK (H300, Sc-22763), and goat polyclonal anti-hScribble (C20, SC 11049) are from Santa Cruz Biotechnology. Rabbit polyclonal anti-Erbin has already been described (32). Anti-PADJ antibody was kindly provided by André Le Bivic (Institut de Biologie du Développement de Marseille Luminy, Marseille, France). Secondary antibodies coupled to horseradish peroxidase and used for Western blotting are from DakoCytomation and The Jackson Laboratory. Secondary antibodies coupled to Alexa fluorophores for immunofluorescent experiments are from Molecular Probes. MDP (Sigma) was used at 50–500 ng/ml.

NF-κB Activation and ELISAs—HEK293T cells were plated at 10⁵ cells/well in 24-well plates and transfected 1 day after with 150 ng of pNF-κB-luciferase Firefly (Clontech), 15 ng of pGL4-TK-luciferase *Renilla* (Promega), and 2–10 ng of NOD2 or RICK pEGFP-expressing plasmid. Transfected cells were stimulated or not for 20–24 h with 50 ng/ml MDP, then lysed in 1× reporter lysis buffer (Promega), and assayed for Firefly luciferase (Yelen Corp.) or for Firefly and *Renilla* luciferase sequentially (Promega). Firefly luciferase values were normalized by dividing by the amount of protein or by the *Renilla* luciferase values. Averages and standard deviations were calculated from duplicate wells using Microsoft Excel. Each experiment was done at least three times.

HEK293T cells were plated at 10⁵ cells/well in 24-well plates, transfected the following day, and then stimulated with MDP ligand for 20–24 h. Cell culture supernatants were collected kept at –20 °C, and IL-8 levels were assayed by ELISA accord-

ing to the manufacturer's instructions (R&D Biosystems or Clinisciences). Supernatants of transiently transfected HEK293T were also analyzed on a Proteoplex 16-well human cytokine array kit (Novagen) to detect in parallel 12 human cytokines. Proteoplex slide was treated and scanned as recommended by the manufacturer.

RESULTS

NOD2 Localizes at the Plasma Membrane of Epithelial Cells—NOD2 is a multimodular protein containing two amino-terminal CARD domains, a central NOD, and a carboxyl-terminal LRR domain (Fig. 1A). To evaluate the subcellular localization of NOD2 in epithelial cells, we expressed EGFP fused to the amino terminus of NOD2 or NOD2 mutants in HEK293T cells and evaluated their expression. Comparable amounts of proteins were detected by Western blot using anti-GFP antibody (Fig. 1A). Activity of EGFP-NOD2 was next assessed by transcriptional assays and ELISAs. Expression of EGFP-NOD2 in HEK293T cells results in an increase of NF-κB activity measured by a κB-luciferase reporter gene in an MDP-dependent manner (Fig. 1B). As expected from previous studies, introduction of the 1007FS, R702W, and G908R mutations within the EGFP-NOD2 sequence impaired with various degrees the MDP-dependent NF-κB transcriptional activity of the protein (Fig. 1B). Although EGFP-NOD2^{1007FS}, a mutant unable to respond to MDP, had basal NF-κB activity, EGFP-NOD2^{R702W} and EGFP-NOD2^{G908R} maintained their inducible NF-κB activity following MDP stimulation, as reported elsewhere (12), albeit with a small decrease in intensity (Fig. 1B). In contrast, no difference is observed in IL-8 secretion between the EGFP-NOD2^{R702W} and EGFP-NOD2^{G908R} mutants and the wild type construct (Fig. 1B). As a control, we also expressed EGFP-NOD2^{LRR} that encompasses the LRRs of NOD2 (Fig. 1A). No NF-κB activity was detected with this construct (data not shown). To correlate the NF-κB transcriptional activity with a biological response, we analyzed the level of different cytokines secreted in the medium of HEK293T cells transfected with EGFP-NOD2 and EGFP-NOD2^{1007FS}. Out of 12 cytokines tested, we only observed a significant increase of IL-8 (supplemental Fig. S1). Therefore, in this cellular model, the NF-κB transcriptional activity of EGFP-NOD2 and its mutants was correlated to the amount of the secreted proinflammatory chemokine interleukine-8 (IL-8) in the supernatants of transfected cells (Fig. 1B). As expected, the release of IL-8 from HEK293T cells transfected with EGFP-NOD2^{1007FS} was not increased following MDP stimulation. Inspection of the localization of the proteins in these cells reveals that EGFP-NOD2 is a membrane-associated protein as shown previously (1). Interestingly, EGFP-NOD2^{1007FS} is no longer found at the plasma membrane and has a cytoplasmic distribution (Fig. 1C), whereas the EGFP-NOD2^{R702W} and EGFP-NOD2^{G908R} mutants are still found at the plasma membrane (data not shown and see Ref. 1). Thus, the loss of inducible NF-κB activity upon MDP treatment of NOD2^{1007FS} is correlated to its loss of membrane localization.

The 1007FS Mutation Impairs the Basolateral Localization of NOD2—We have already shown that NOD2 is localized basolaterally in polarized Caco-2 cells (2). We confirm here by using another well recognized model of polarized epithelial cells

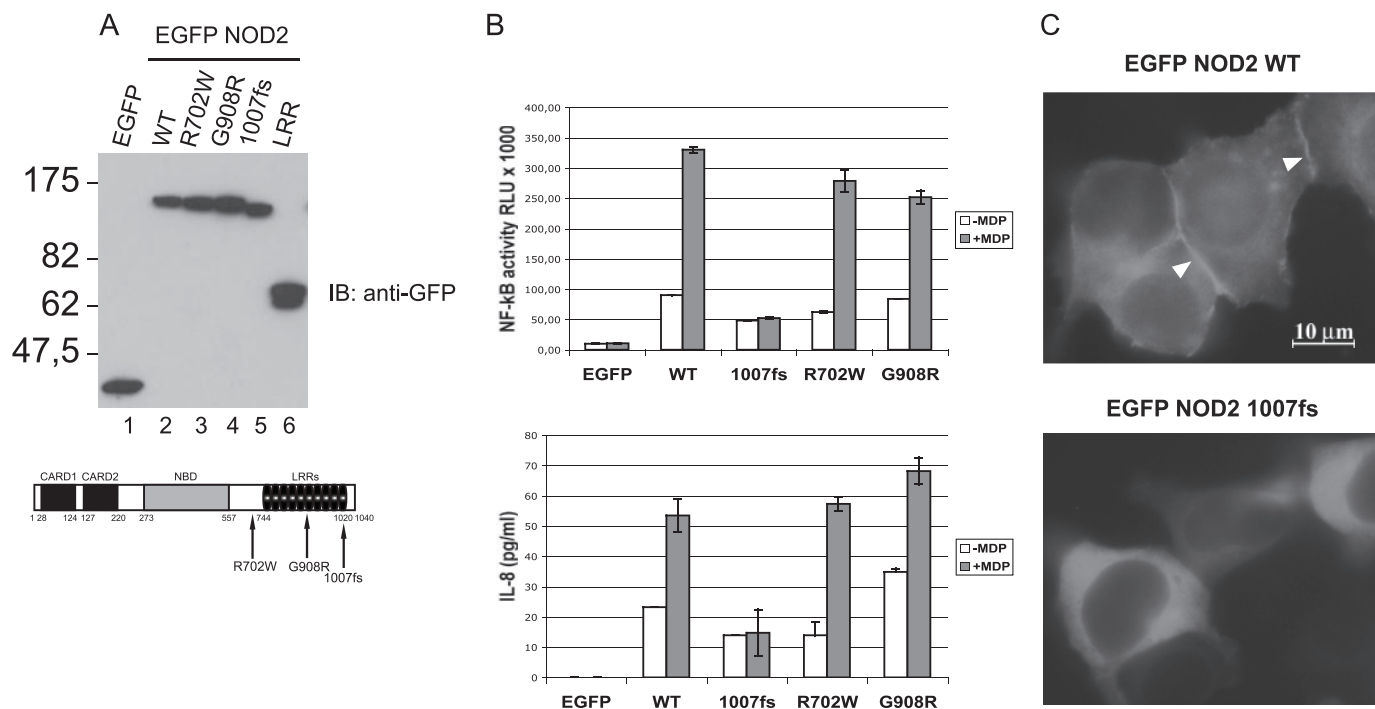


FIGURE 1. **EGFP-NOD2 WT but not EGFP-NOD2^{1007FS} localized to the plasma membrane in HEK293T cells.** Expression, IL-8 secretion, NF-κB activity, and localization of EGFP-NOD2 WT and CD-associated mutants are shown. *A*, protein expression analysis by immunoblotting (IB) of whole cell lysates from HEK293T cells transiently transfected with EGFP-NOD2 WT (lane 2), EGFP-NOD2 CD-associated mutants (lanes 3–5), or the LRRs alone (lane 6). A schematic representation of NOD2 shows the localization of the CD-associated mutations within the protein. *B*, NF-κB activation (top) and IL-8 secretion (bottom) in HEK293T cells transiently transfected with EGFP-NOD2 wild type or CD-associated EGFP-NOD2 variants with or without MDP stimulation. *C*, fluorescence of HEK293T cells transiently transfected with wild type EGFP-NOD2 or EGFP-NOD2^{1007FS} plasmids. Arrows indicate the membrane-bound NOD2 protein.

(MDCKII) that EGFP-NOD2 is localized at the basolateral membrane compartment and that the NOD2^{1007FS} mutation abrogates this membrane localization (supplemental Fig. S2).

Activity of myr-EGFP-NOD2 and myr-EGFP-NOD2FS—Barnich *et al.* (1) have proposed that the presence of NOD2 at the plasma membrane is a prerequisite of its NF-κB activity. If so, targeting of NOD2 at the plasma membrane should provide a maximal activation of the protein. We thus constructed a myristoylated version of EGFP-NOD2 by fusing the first 11 amino acids of Lck to EGFP (myr-EGFP-NOD2) and transfected HEK293T cells to study the localization and the activity of the myristoylated protein. This construct strongly localizes at the plasma membrane in cells in contrast to EGFP-NOD2, which is more weakly found at the cell periphery and more abundant in the cytosol (Fig. 2*A* and data not shown). However, overexpression of myr-EGFP-NOD2 exhibits NF-κB activity comparable with the nonmyristoylated form as indicated by the luciferase NF-κB reporter assay and IL-8 secretion (Fig. 2, *B* and *C*). Because enforcing the plasma membrane localization of NOD2 has only a slight effect on basal NF-κB activity and induction upon MDP stimulation, we can conclude that a limiting factor prevents a further increased activity of the myristoylated EGFP-NOD2 at the plasma membrane. Because EGFP-NOD2^{1007FS} does not localize at the plasma membrane, we ask the question whether enforcing EGFP-NOD2^{1007FS} localization to the plasma membrane may rescue its MDP response. The myristoylated EGFP-NOD2^{1007FS} protein was expressed in HEK293T cells, and NF-κB transcriptional activity as well as IL-8 secretion were measured (Fig. 2, *C* and *D*). Although myr-EGFP-NOD2^{1007FS} is readily found at the plasma membrane

(Fig. 2*A*), it is unable to induce NF-κB transcriptional activity or IL-8 secretion in response to MDP (Fig. 2, *C* and *D*). Therefore, the impaired NF-κB transcriptional activity of EGFP-NOD2^{1007FS} in response to MDP is not linked to its cytosolic localization but rather to its inability to recognize MDP. Surprisingly, the ability of the myr-EGFP-NOD2^{1007FS} mutant to induce NF-κB and mostly to produce IL-8 is decreased compared with the nonmyristoylated protein (Fig. 2, *B* and *C*). This suggests that membrane localization of NOD2^{1007FS} may have a negative effect on IL-8 production through a signaling pathway different from the NF-κB signaling. Membrane targeting of the other different CD-associated mutants (R702W and G908R) and the Blau mutant (R334Q) of NOD2 by myristoylation has little if any effect on NF-κB transcriptional activity and IL-8 production (Fig. 2*D* and data not shown). From these experiments we can conclude that membrane targeting of EGFP-NOD2 and the CD-associated mutants R702W and G908R does not modify their activities (NF-κB transcriptional activity and IL-8 secretion). In contrast, targeting EGFP-NOD^{1007FS} to the plasma membrane decreases its ability to induce NF-κB activity and mostly IL-8 secretion.

Recruitment of RICK at the Plasma Membrane Enhances the NF-κB Transcriptional Activity—The lack of increased NF-κB activity by expression of myr-EGFP-NOD2 could be explained by the limited amount of an endogenous factor required for NOD2-dependent NF-κB activation at the plasma membrane. RICK is a good candidate because NOD2 activity is dependent on its interaction with this serine-threonine kinase via a homophilic CARD-CARD interaction (10). We therefore expressed a myr-EGFP-tagged version of RICK in HEK293T

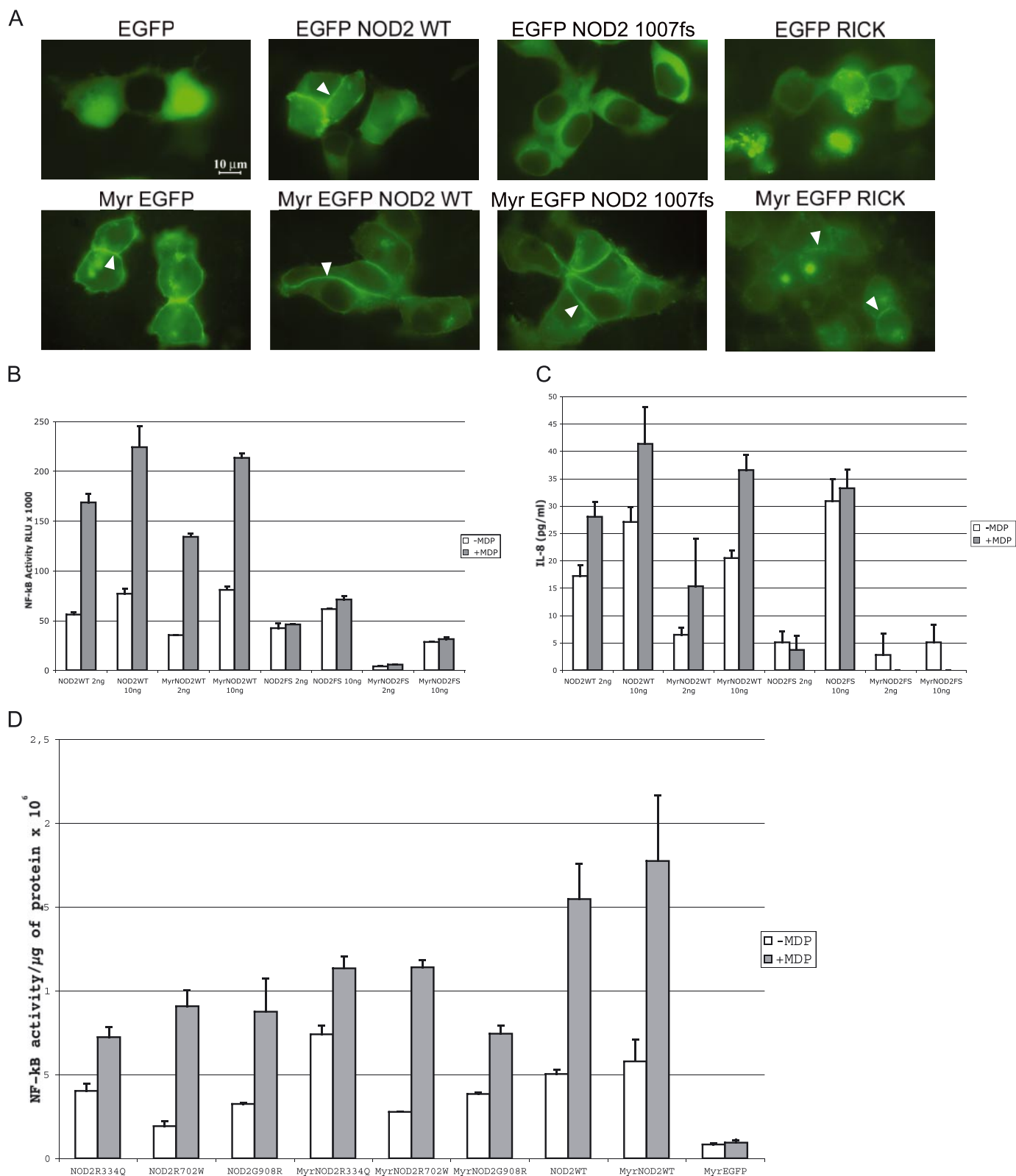
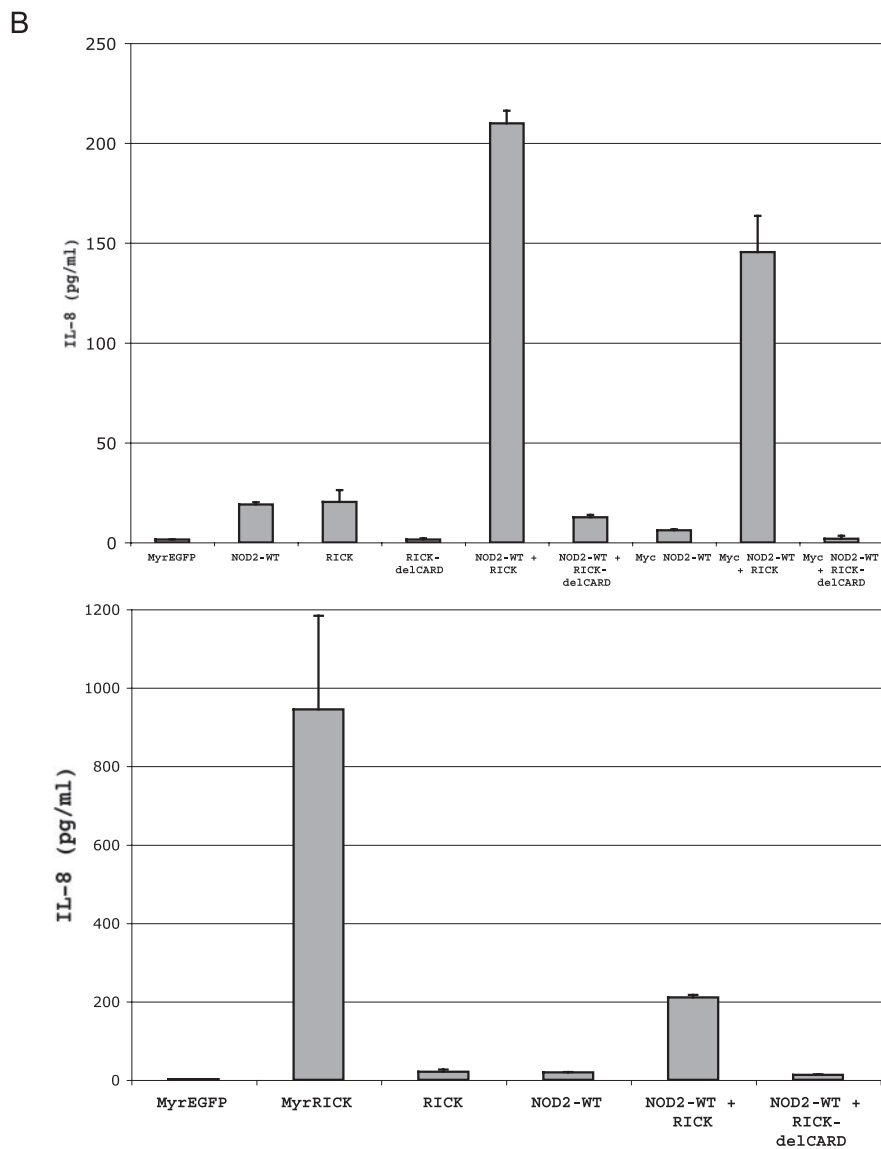
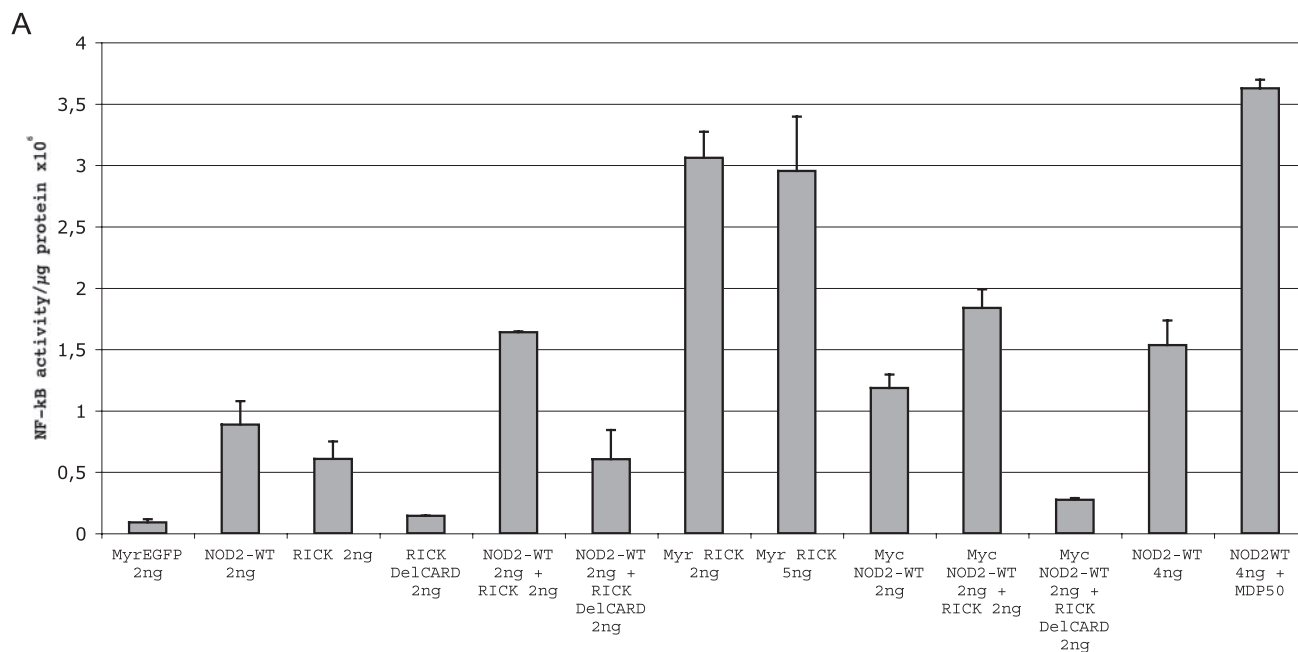


FIGURE 2. Enforced localization of EGFP-NOD2 WT to the plasma membrane does not modify its NF- κ B activity or IL-8 secretion. *A*, fluorescence analysis of HEK293T cells transiently transfected with EGFP constructs targeted or not to the plasma membrane by a myristoylation site (*myr*). The white arrowheads indicate plasma membrane localization. *B* and *C*, NF- κ B activity and IL-8 secretion of EGFP-NOD2 WT and EGFP-NOD2^{1007FS} myristoylated or not with or without MDP stimulation (50 ng/ml). Transient transfections were performed with 2 and 10 ng of each EGFP plasmid. *D*, NF- κ B activity of HEK293T cells transiently expressing EGFP-NOD2 WT, CD-associated mutants R702W, G908R, and Blau mutant R334Q myristoylated or not with or without MDP stimulation. Transient transfections were done with 5 ng of each EGFP plasmid.

Membrane Signaling of NOD2 and RICK



cells and verified its subcellular localization (Fig. 2A). Although EGFP-RICK protein tends to accumulate in aggregates in the cytoplasm and is not detected at the plasma membrane, the myristoylated form expressed in HEK293T cells is readily localized at the plasma membrane (Fig. 2A). Expression of myr-EGFP-RICK results in a strong NF- κ B activation compared with the basal activity of the nonmyristoylated form (EGFP-RICK) (Fig. 3A). Increased IL-8 secretion is also observed when targeting RICK to the plasma membrane. However, the difference between myr-EGFP-RICK and EGFP-RICK is much more pronounced when considering IL-8 secretion (Fig. 3B). An increase in NF- κ B transcriptional activity and IL-8 secretion is also observed when coexpressing NOD2 and RICK, although NF- κ B activity is less pronounced than when RICK is targeted to the plasma membrane by myristoylation, suggesting that membrane recruitment is an important step in RICK activation. The synergy of activation between NOD2 and RICK is observed with two different tagged versions of NOD2 (EGFP or Myc) and required a NOD2-RICK interaction because it did not occur with the ECFP-RICK Δ CARD (Fig. 3, A and B). NF- κ B activity and IL-8 secretion induced by myr-EGFP-NOD2 are inhibited by coexpressing an ECFP-RICK Δ CARD construct but not by coexpressing a myr-EGFP-NOD2^{1007FS} showing that, unlike RICK Δ CARD, myr-EGFP-NOD2^{1007FS} does not function as a dominant negative protein for myr-EGFP-NOD2 (supplemental Fig. S3). In addition, myr-EGFP-RICK activity is insensitive to the coexpression of either RICK Δ CARD or myr-EGFP-NOD2^{1007FS} (supplemental Fig. S3). Altogether these results show that localizing RICK at the plasma membrane by myristoylation induces a very efficient NF- κ B signaling triggering a large IL-8 secretion. As a pool of NOD2 is localized at the plasma membrane, these data also suggest that the function of NOD2 could be to recruit RICK at the plasma membrane to form an active complex able to activate part of the NF- κ B pathway.

RICK Is Recruited at the Plasma Membrane in a NOD2-dependent Manner—To test this hypothesis, we evaluated the subcellular localization of RICK by immunofluorescence in the presence or absence of NOD2. Expression of Myc-NOD2, but not of a Myc-CblA protein control, induces the recruitment of RICK at the plasma membrane in HEK293T cells suggesting that NOD2 may act as an anchor for the serine-threonine kinase (Fig. 4A). To confirm this hypothesis, HCT116 colonic epithelial cells were transfected with ECFP-RICK alone or with Myc-NOD2 (Fig. 4B) providing the same recruitment of RICK at the plasma membrane.

To confirm that NOD2 is able to recruit RICK at the plasma membrane, biochemical fractionation experiments were performed in HEK293T cells transfected with various NOD2 GFP-tagged constructs (Fig. 5). Immunoblot analysis showed that EGFP-NOD2 and mostly myr-EGFP-NOD2, a plasma mem-

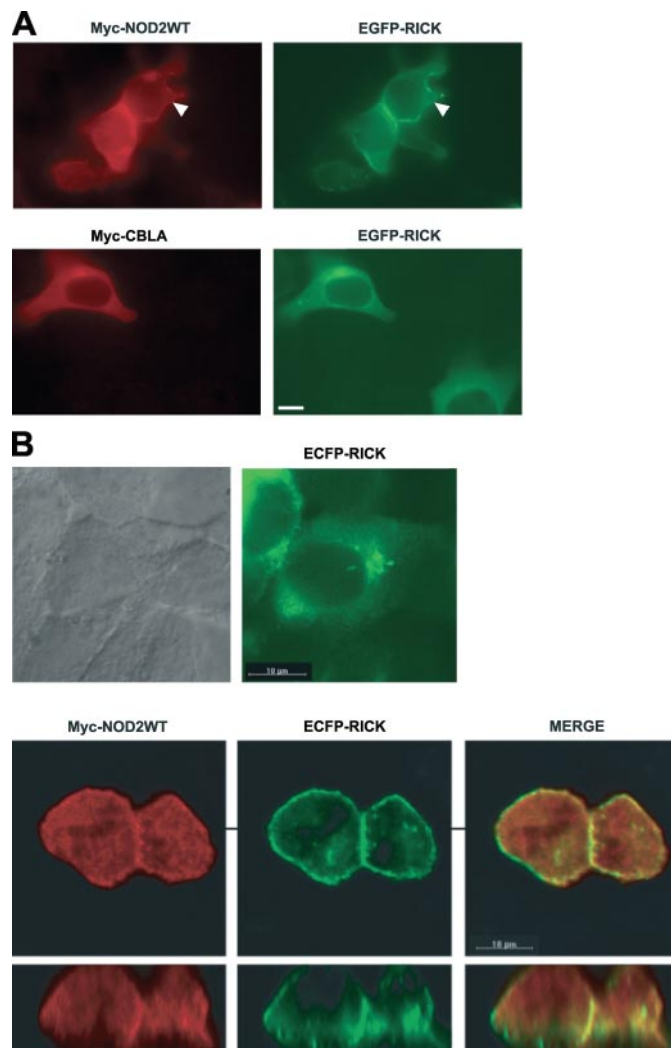


FIGURE 4. Myc-NOD2 is able to recruit ECFP-RICK to the plasma membrane in HEK293T cells and in HCT116. A, immunofluorescence analysis of HEK293T cells coexpressing either Myc-NOD2 WT and EGFP-RICK (top) or Myc-CBLA and EGFP-RICK (bottom). White arrowhead denotes plasma membrane localization. The scale bar is 10 μ m long. B, immunofluorescence analysis of HCT116 colonic cells expressing ECFP-RICK (top right) or coexpressing Myc-NOD2 WT and ECFP-RICK (bottom). Images of cells coexpressing Myc-NOD2 WT and ECFP-RICK were deconvoluted with Imaris software (Bitplane) and are displayed in the XY and XZ field. From left to right are shown the labeling of NOD2, RICK, and merge.

brane targeted NOD2 protein (Fig. 2), are present in a Triton X-100-insoluble fraction (Fig. 5A, left panel, lanes 6 and 12). Similarly, myr-EGFP-RICK, which is localized at the plasma membrane by immunofluorescence (Fig. 2), is enriched in this Triton X-100-insoluble fraction compared with a nonmyristoylated RICK version (Fig. 5A, right panel, compare lanes 3 and 6). These results indicate that this Triton X-100-insoluble fraction is enriched in plasma membrane-localized proteins. An enrichment of endogenous RICK is observed in this Triton X-100-

FIGURE 3. Enforced localization of EGFP-RICK to the plasma membrane increased its NF- κ B activity and IL-8 secretion. A, NF- κ B activity of EGFP-RICK or myristoylated EGFP-RICK in HEK293T cells transiently transfected with the indicated amount of expressing vectors. As a comparison, NF- κ B activities of HEK293T cells expressing EGFP-NOD2 WT or coexpressing EGFP-NOD2WT and EGFP-RICK or EGFP-RICK Δ CARD are shown. Myc-tagged NOD2 expression vectors are also used to show that the epitope tag does not modify the NF- κ B response. B, IL-8 secretion (top) analysis of HEK293T supernatants transiently transfected by the indicated expression vector showing that the synergy observed when coexpressing NOD2 WT and RICK is dependent upon the presence of the RICK CARD domain. IL-8 ELISA (bottom) analysis highlights the increase of IL-8 secretion of HEK293T cells expressing Myr EGFP-RICK compared with EGFP-RICK.

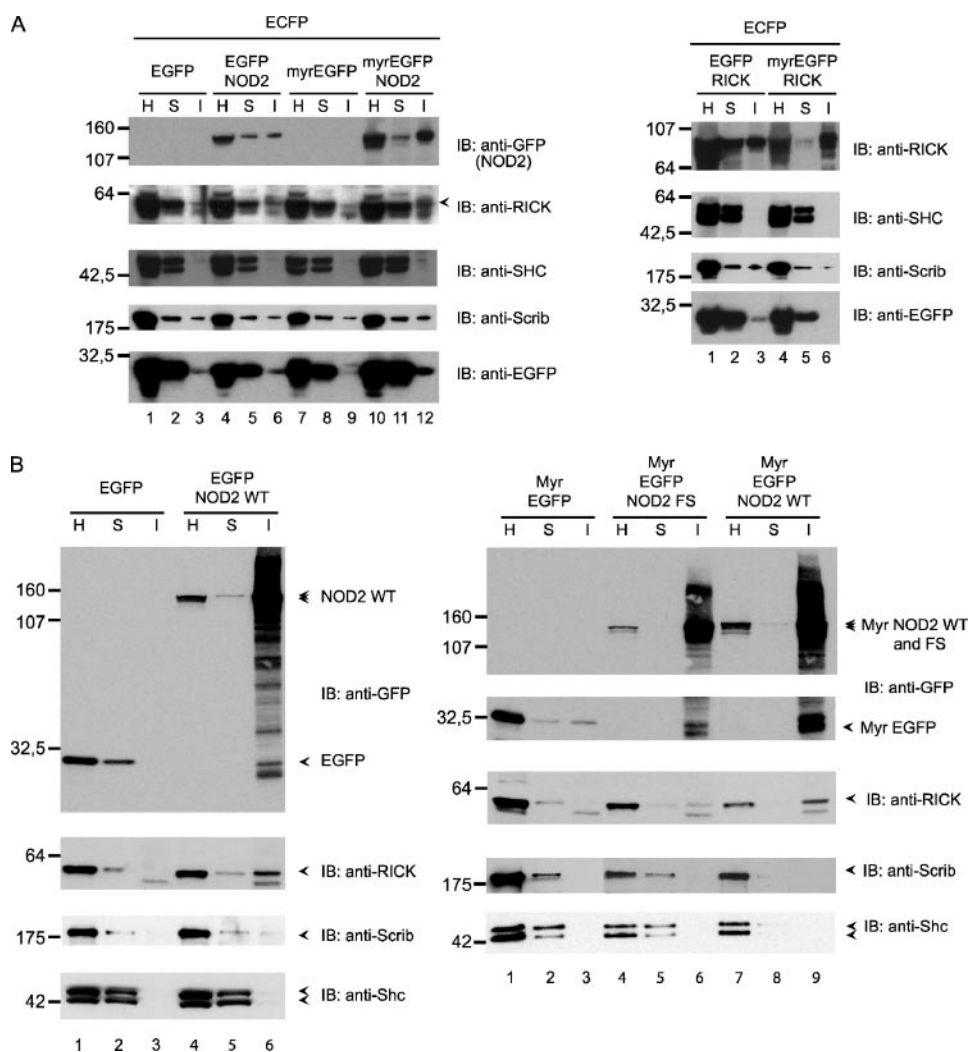


FIGURE 5. Biochemical fractionation of HEK293T cells confirms the plasma membrane recruitment of RICK by NOD2. *A*, HEK293T cells transiently transfected with EGFP-NOD2 (lanes 4–6), myr-EGFP-NOD2 (lanes 10–12), or control plasmids EGFP (lanes 1–3) and myr-EGFP (lanes 7–9) (left panel) and with EGFP-RICK (lanes 1–3) and myr-EGFP-RICK (lanes 4–6) (right panel) were used for biochemical fractionation. Immunoblot (IB) analysis with anti-GFP, anti-RICK, anti-hScribble and anti-Shc antibodies were realized on the hypotonic (H), Triton X-100 soluble (S), and Triton X-100-insoluble (I) fractions. *B*, biochemical cell fractionation experiment was performed with HEK293T cells as in *A* with EGFP or EGFP-NOD2 (left panel) and myr-EGFP, myr-EGFP NOD2, and myr-EGFP-NOD2^{FS} (right panel). Immunoblot analysis with anti-GFP, anti-RICK, anti-hScribble, and anti-Shc were realized on the hypotonic (H), Triton X-100-soluble (S) and Triton X-100-insoluble (I) fractions.

insoluble fraction following EGFP-NOD2 expression (Fig. 5, *A*, left panel, compare lanes 3 and 6, and *B*, left panel, compare lanes 3 and 6), and this phenomenon is enhanced with myr-EGFP-NOD2 expression (Fig. 5, *A*, left panel, compare lanes 9 and 12, and *B*). In contrast, little amount of endogenous RICK is seen in this insoluble fraction from cells overexpressing EGFP (Fig. 5, *A*, left panel, lanes 3 and 9, and *B*, left panel, lanes 3 and 6) or myr-EGFP control proteins (Fig. 5*B*, right panel compare lanes 3 and 9). Other endogenous proteins Scribble and Shc are, respectively, either not enriched or are not detected in the Triton X-100-insoluble fraction indicating that the recruitment of endogenous RICK by NOD2 into this fraction is specific. The recruitment of endogenous RICK is also seen with a plasma membrane-targeted NOD2^{FS} protein, myr-EGFP-NOD2^{1007FS}, although less strongly than with myr-EGFP-NOD2, which confirms the work of Abbott *et al.* (15) showing that NOD2^{FS} interacts less strongly with RICK than NOD2^{WT}. Altogether these

biochemical results are consistent with our immunofluorescence data showing that overexpressing NOD2 leads to a membrane recruitment of RICK.

To strengthen this result we carried out an additional fluorescent microscopic analysis of HCT116 cells coexpressing other fluorescent forms of NOD2 and RICK, *i.e.* EYFPNOD2 and ECFPRICK (Fig. 6). These two different fluorescent GFPs were selected by virtue of their strictly nonoverlapping emission spectra to obtain an unambiguous analysis of NOD2 and RICK localization. Furthermore, cells transfected with only GFP-derived plasmids do not require permeabilization or specific treatment that may result in labeling artifacts. HCT116 cells were cotransfected with various combinations of EYFP-NOD2 and ECFP-RICK constructs encoding full-length or deleted versions of these proteins. Membrane recruitment of ECFP-RICK by EYFP-NOD2 is readily observed when both full-length proteins are expressed in the same HCT116 cell (Fig. 6, *arrows*). A reconstituted image in the XZ plan shows that EYFP-NOD2 and ECFP-RICK colocalize in membrane notably at the junction between two cells (Fig. 6). Furthermore, this recruitment is dependent upon a specific CARD-CARD interaction because an ECFP-RICK Δ CARD mutant is not recruited to the plasma membrane by EYFP-NOD2 contrasting with an ECFP-RICK Δ KINASE (containing the CARD domain) that is efficiently recruited at the plasma membrane by EYFP-NOD2. Conversely, we demonstrate that the CARDS domains of NOD2 do not localize at the plasma membrane and do not induce a membrane recruitment of RICK (Fig. 6).

Localization of Endogenous RICK at the Plasma Membrane of THP1 Cells—Because of low level of expression, endogenous NOD2 is difficult to detect by immunofluorescence. Nevertheless, NOD2 has been observed at the plasma membrane of the colonic HT29 cell line (1, 30). To our knowledge, however, no studies have yet been reported concerning the localization of endogenous RICK protein. To reinforce our *in vitro* data, we investigated the subcellular localization of RICK in the monocytic cell line THP1. MDP stimulation induces an efficient secretion of IL-8 in THP1 cells, and we confirm that these cells express NOD2 (data not shown) (33). We show by immunoblot

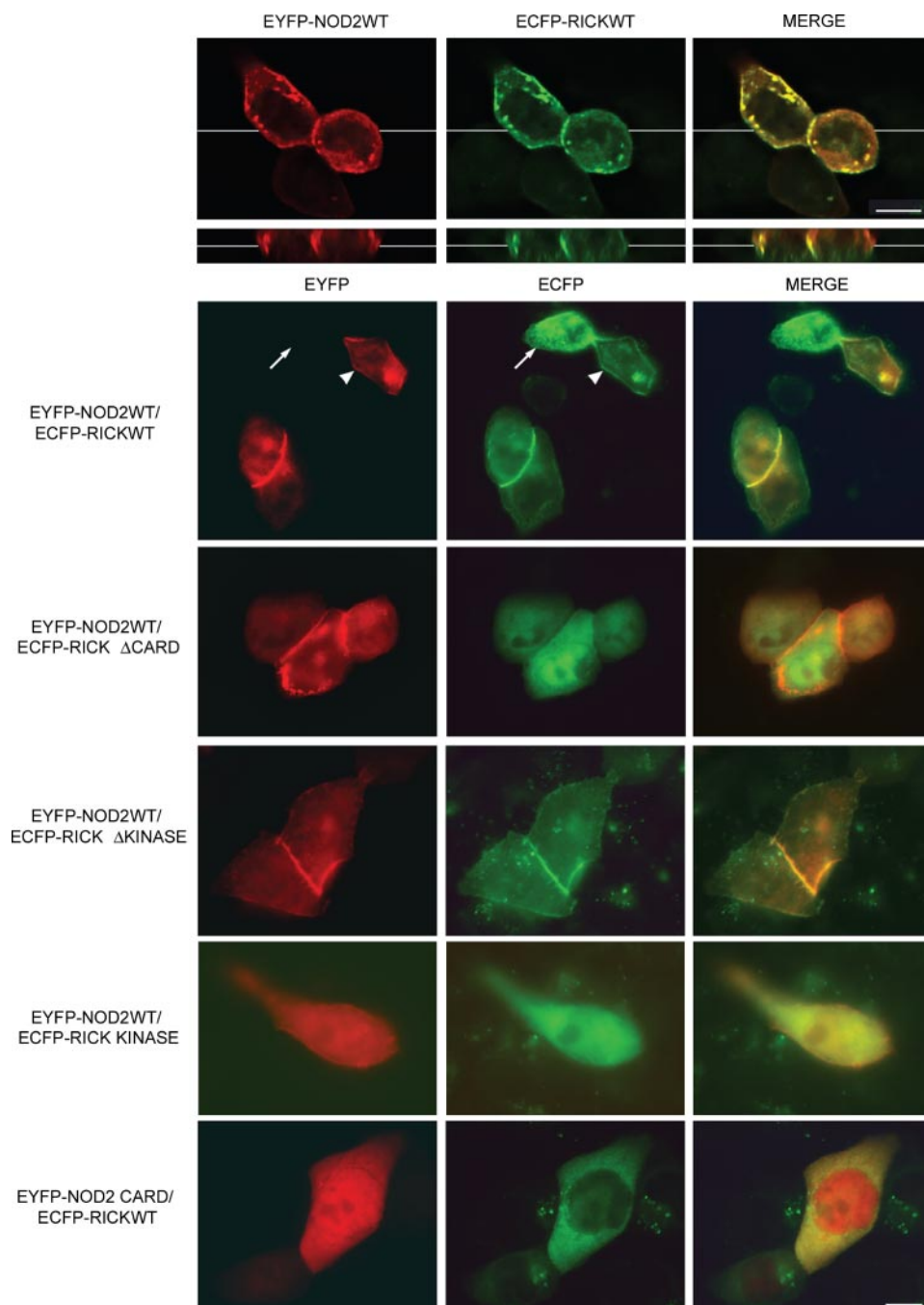


FIGURE 6. Plasma membrane recruitment of RICK by NOD2 depends upon the presence of its CARD domain. *Top*, immunofluorescence analysis of HCT116 colonic cells coexpressing EYFP-NOD2 and ECFP-RICK. Images of cells coexpressing EYFP-NOD2WT and ECFP-RICK were deconvoluted with Imaris software (Bitplane) and are displayed in the XY and XZ field. From left to right are shown the labeling of NOD2, RICK, and merge. The scale bar represents 10 μ m. *Bottom*, fluorescence analysis showing EYFP (left), ECFP (middle), and merge images (right) of HCT116 colonic cells coexpressing various combinations of EYFP-NOD2 and ECFP-RICK constructs. ECFP-RICK is recruited at the plasma membrane in cells coexpressing EYFP-NOD2 (white arrowheads), whereas cells expressing only ECFP-RICK display no membrane staining (white arrows). The scale bar represents 10 μ m.

that RICK is also expressed in THP1 cells (Fig. 7). Immunofluorescence analysis revealed that endogenous RICK is indeed detected at the plasma membrane of THP1 cells (Fig. 7).

DISCUSSION

In this study we have investigated the impact of the subcellular localization of NOD2 and RICK on NF- κ B signaling and

IL-8 secretion. We confirmed that NOD2 is associated with the plasma membrane in HEK293T cells and in the MDCKII-polarized epithelial cell line. Recently, a correlation between plasma membrane localization of NOD2 and efficient NF- κ B activity has been shown (1). Here we have designed experiments to test the ability of NOD2 to activate IL-8 secretion from the plasma membrane. We demonstrate by enforcing membrane localization of NOD2 that this protein is active at the plasma membrane. Furthermore, we show that NOD2 induces a membrane recruitment of RICK that is dependent on a CARD-CARD interaction.

Activity of Membrane-targeted NOD2^{1007ES} Mutant—Among the three most common mutants found in CD, the NOD2^{1007ES} mutant is the only one to be unresponsive to MDP and to be delocalized in the cytoplasm (this study) (1). Targeting the NOD2^{1007ES} mutant to the plasma membrane did not restore a MDP response and has apparently no effect on basal NF- κ B transcriptional activity. IL-8 secretion appears lowered, however, when expressing the myristoylated NOD2^{1007ES} compared with its nonmyristoylated form. This finding probably reflects a signaling deficiency of membrane-bound NOD2^{1007ES}. Indeed, we did not observe a dominant negative activity of myristoylated NOD2^{1007ES} on NOD2 or RICK signaling at least when considering NF- κ B luciferase and IL-8 secretion readouts. Our studies confirm other works using protein overexpression in HEK293 cells (1, 12, 22) and suggest that the NOD2^{1007ES} protein behaves as a defective mutant unable to respond to MDP.

NOD2 Signaling and IL-8 Secretion—IL-8 gene transcription depends on NF- κ B activation in every cell type but also on the complex interplay of other transcription factors such as AP-1 and CEBP upon stimulation of MAPKs (extracellular signal-regulated kinase (ERK), p38 MAPK, and c-Jun NH₂-terminal kinase (JNK)) for maximum induction (34–37). It is known that AP1 sites in the IL-8 promoter can temporally integrate early positive and delayed neg-

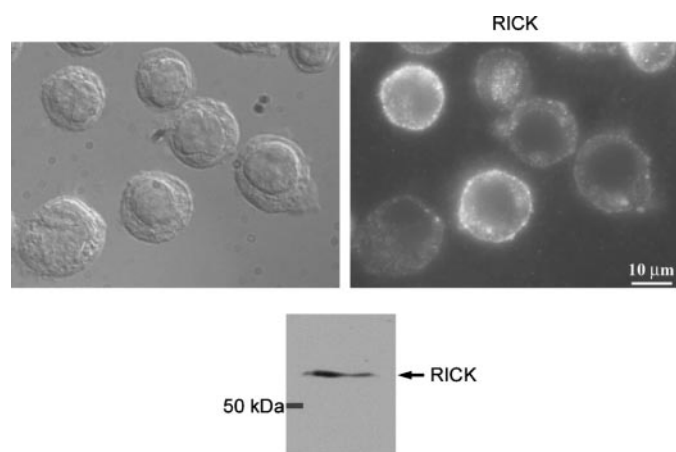


FIGURE 7. Endogenous RICK proteins localized at the membrane of THP1 monocytic cell line. Immunofluorescence of THP1 cells revealed with an anti-RICK rabbit polyclonal antibody (H300; Sc-22763, Santa Cruz Biotechnology). Nomarski view and immunofluorescence labeling of the same field are given side by side. Immunoblot analysis of a THP1 Triton cell lysate revealed with the same anti-RICK rabbit polyclonal antibody was used for immunofluorescence labeling.

active effects on *IL-8* gene transcription depending on the relative binding of c-Fos and Fra1, respectively (34). The effect of membrane localization of NOD2 on MAPK-dependent transcription factors awaits further investigation. In this regard, we and other have shown that Erbin, a basolateral protein known to be involved in MAPK regulation, interacts with NOD2 and down-regulates NF- κ B activity upon MDP stimulation (2, 30, 38–40). Moreover, basolateral membrane localization of NOD2 is not affected by Erbin short interfering RNA arguing against a role of Erbin as an anchor for NOD2 at the plasma membrane but more likely as a signaling or scaffolding component of the NOD2-RICK protein complex in epithelial cells (data not shown) (30). Because delocalized NOD2^{1007FS} no longer binds to Erbin, it is possible that the cytoplasmic NOD2^{1007FS} mutant is not negatively regulated by Erbin and induces unregulated signaling from the cytosol.

Activation of RICK at the Plasma Membrane—Our work suggests that RICK activity depends on its membrane localization. First, the enforced association of RICK with the plasma membrane strongly stimulates NF- κ B activity and *IL-8* production. Second, NOD2 is able to recruit RICK at the membrane through a CARD-CARD interaction. Third, we observe an endogenous RICK localization at the plasma membrane in THP1 cells. Therefore, NOD2 may control NF- κ B signalization by regulating the pool of RICK recruited at the plasma membrane. Whether other NOD proteins such as NOD1 are also able to activate and recruit RICK at the membrane remains to be evaluated. This membrane compartmentalization mechanism resembles what has been described for integral membrane TLRs and tumor necrosis factor α receptor to regulate downstream signalization (41–43). NOD2 could exert a negative effect on TLR2 signaling in sequestering a limiting factor of signaling such as RICK (23, 44). In such a case, by its delocalization and its lack of response to MDP, the NOD2^{1007FS} mutant would not be able to properly modulate TLR2 signalization and will instead induce the production of an excess of proinflammatory cytokines.

In conclusion our data highlight novel findings on the modalities of NOD2 activation and reveal a mechanism of membrane recruitment of RICK depending on NOD2. Elucidating the signaling routes initiated from the plasma membrane by the NOD2-RICK complex and their coordinated interplay as well as their cell specificity will be a major challenge to understand the biological role of NOD2 in normal and pathological conditions.

Acknowledgments—We thank Nicolas Vidal (Yelen Corp.) for luciferase assays, Alain Bernadac for microscopy analysis, Patrice Dubreuil for THP1 cells, Claude Mawas for helpful comments on the manuscript, and all members of UMR INRA1111 and UMR599 INSERM labs for their help.

REFERENCES

- Barnich, N., Aguirre, J. E., Reinecker, H. C., Xavier, R., and Podolsky, D. K. (2005) *J. Cell Biol.* **170**, 21–26
- McDonald, C., Chen, F. F., Ollendorff, V., Ogura, Y., Marchetto, S., Lecine, P., Borg, J. P., and Nunez, G. (2005) *J. Biol. Chem.* **280**, 40301–40309
- Inohara, N., Chamaillard, M., McDonald, C., and Nunez, G. (2005) *Annu. Rev. Biochem.* **74**, 355–383
- Russell, R. K., Nimmo, E. R., and Satsangi, J. (2004) *Curr. Opin. Genet. Dev.* **14**, 264–270
- Gaya, D. R., Russell, R. K., Nimmo, E. R., and Satsangi, J. (2006) *Lancet* **367**, 1271–1284
- Hugot, J. P., Chamaillard, M., Zouali, H., Lesage, S., Cezard, J. P., Belaiche, J., Almer, S., Tysk, C., O'Morain, C. A., Gassull, M., Binder, V., Finkel, Y., Cortot, A., Modigliani, R., Laurent-Puig, P., Gower-Rousseau, C., Macry, J., Colombel, J. F., Sahbatou, M., and Thomas, G. (2001) *Nature* **411**, 599–603
- Ogura, Y., Bonen, D. K., Inohara, N., Nicolae, D. L., Chen, F. F., Ramos, R., Britton, H., Moran, T., Karaliuskas, R., Duerr, R. H., Achkar, J. P., Brant, S. R., Bayless, T. M., Kirschner, B. S., Hanauer, S. B., Nunez, G., and Cho, J. H. (2001) *Nature* **411**, 603–606
- Economou, M., Trikalinos, T. A., Loizou, K. T., Tsianos, E. V., and Ioannidis, J. P. (2004) *Am. J. Gastroenterol.* **99**, 2393–2404
- Inohara, N., and Nunez, G. (2003) *Nat. Rev. Immunol.* **3**, 371–382
- Ogura, Y., Inohara, N., Benito, A., Chen, F. F., Yamaoka, S., and Nunez, G. (2001) *J. Biol. Chem.* **276**, 4812–4818
- Girardin, S. E., Boneca, I. G., Viala, J., Chamaillard, M., Labigne, A., Thomas, G., Philpott, D. J., and Sansonetti, P. J. (2003) *J. Biol. Chem.* **278**, 8869–8872
- Inohara, N., Ogura, Y., Fontalba, A., Gutierrez, O., Pons, F., Crespo, J., Fukase, K., Inamura, S., Kusumoto, S., Hashimoto, M., Foster, S. J., Moran, A. P., Fernandez-Luna, J. L., and Nunez, G. (2003) *J. Biol. Chem.* **278**, 5509–5512
- Tanabe, T., Chamaillard, M., Ogura, Y., Zhu, L., Qiu, S., Masumoto, J., Ghosh, P., Moran, A., Predergast, M. M., Tromp, G., Williams, C. J., Inohara, N., and Nunez, G. (2004) *EMBO J.* **23**, 1587–1597
- Inohara, N., Koseki, T., Lin, J., del Peso, L., Lucas, P. C., Chen, F. F., Ogura, Y., and Nunez, G. (2000) *J. Biol. Chem.* **275**, 27823–27831
- Abbott, D. W., Wilkins, A., Asara, J. M., and Cantley, L. C. (2004) *Curr. Biol.* **14**, 2217–2227
- Rogler, G., Brand, K., Vogl, D., Page, S., Hofmeister, R., Andus, T., Knuechel, R., Baeuerle, P. A., Scholmerich, J., and Gross, V. (1998) *Gastroenterology* **115**, 357–369
- Schreiber, S., Nikolaus, S., and Hampe, J. (1998) *Gut* **42**, 477–484
- Maeda, S., Hsu, L. C., Liu, H., Bankston, L. A., Iimura, M., Kagnoff, M. F., Eckmann, L., and Karin, M. (2005) *Science* **307**, 734–738
- Kobayashi, K. S., Chamaillard, M., Ogura, Y., Henegariu, O., Inohara, N., Nunez, G., and Flavell, R. A. (2005) *Science* **307**, 731–734
- van Heel, D. A., Ghosh, S., Butler, M., Hunt, K. A., Lundberg, A. M., Ahmad, T., McGovern, D. P., Onnie, C., Negoro, K., Goldthorpe, S., Foxwell, B. M., Mathew, C. G., Forbes, A., Jewell, D. P., and Playford, R. J.

- (2005) *Lancet* **365**, 1794–1796
21. Netea, M. G., Kullberg, B. J., de Jong, D. J., Franke, B., Sprong, T., Naber, T. H., Drenth, J. P., and van der Meer, J. W. (2004) *Eur. J. Immunol.* **34**, 2052–2059
 22. Bonen, D. K., Ogura, Y., Nicolae, D. L., Inohara, N., Saab, L., Tanabe, T., Chen, F. F., Foster, S. J., Duerr, R. H., Brant, S. R., Cho, J. H., and Nunez, G. (2003) *Gastroenterology* **124**, 140–146
 23. Watanabe, T., Kitani, A., Murray, P. J., and Strober, W. (2004) *Nat. Immun.* **5**, 800–808
 24. Martinon, F., and Tschopp, J. (2005) *Trends Immunol.* **26**, 447–454
 25. Eckmann, L., and Karin, M. (2005) *Immunity* **22**, 661–667
 26. Ogura, Y., Lala, S., Xin, W., Smith, E., Dowds, T. A., Chen, F. F., Zimmermann, E., Tretiakova, M., Cho, J. H., Hart, J., Greenson, J. K., Keshav, S., and Nunez, G. (2003) *Gut* **52**, 1591–1597
 27. Chen, C. M., Gong, Y., Zhang, M., and Chen, J. J. (2004) *J. Biol. Chem.* **279**, 25876–25882
 28. Barnich, N., Hisamatsu, T., Aguirre, J. E., Xavier, R., Reinecker, H. C., and Podolsky, D. K. (2005) *J. Biol. Chem.* **280**, 19021–19026
 29. Damiano, J. S., Oliveira, V., Welsh, K., and Reed, J. C. (2004) *Biochem. J.* **381**, 213–219
 30. Kufer, T. A., Kremmer, E., Banks, D. J., and Philpott, D. J. (2006) *Infect. Immun.* **74**, 3115–3124
 31. Simpson, J. C., Wellenreuther, R., Poustka, A., Pepperkok, R., and Wiemann, S. (2000) *EMBO Rep.* **1**, 287–292
 32. Borg, J. P., Marchetto, S., Le Bivic, A., Ollendorff, V., Jaulin-Bastard, F., Saito, H., Fournier, E., Adelaide, J., Margolis, B., and Birnbaum, D. (2000) *Nat. Cell Biol.* **2**, 407–414
 33. Uehara, A., Yang, S., Fujimoto, Y., Fukase, K., Kusumoto, S., Shibata, K., Sugawara, S., and Takada, H. (2005) *Cell Microbiol.* **7**, 53–61
 34. Hoffmann, E., Thiefes, A., Buhrow, D., Dittrich-Breiholz, O., Schneider, H., Resch, K., and Kracht, M. (2005) *J. Biol. Chem.* **280**, 9706–9718
 35. Hoffmann, E., Dittrich-Breiholz, O., Holtmann, H., and Kracht, M. (2002) *J. Leukocyte Biol.* **72**, 847–855
 36. Nourbakhsh, M., Kalble, S., Dorrie, A., Hauser, H., Resch, K., and Kracht, M. (2001) *J. Biol. Chem.* **276**, 4501–4508
 37. Chinenov, Y., and Kerppola, T. K. (2001) *Oncogene* **20**, 2438–2452
 38. Kolch, W. (2003) *Sci. STKE* **2003**, PE37
 39. Huang, Y. Z., Zang, M., Xiong, W. C., Luo, Z., and Mei, L. (2003) *J. Biol. Chem.* **278**, 1108–1114
 40. Dai, P., Xiong, W. C., and Mei, L. (2006) *J. Biol. Chem.* **281**, 927–933
 41. Strober, W., Murray, P. J., Kitani, A., and Watanabe, T. (2006) *Nat. Rev. Immunol.* **6**, 9–20
 42. Liew, F. Y., Xu, D., Brint, E. K., and O'Neill, L. A. (2005) *Nat. Rev. Immunol.* **5**, 446–458
 43. Ea, C. K., Deng, L., Xia, Z. P., Pineda, G., and Chen, Z. J. (2006) *Mol. Cell* **22**, 245–257
 44. Kobayashi, K., Inohara, N., Hernandez, L. D., Galan, J. E., Nunez, G., Janeway, C. A., Medzhitov, R., and Flavell, R. A. (2002) *Nature* **416**, 194–199